Reactions of the Dirhenium(II) Complexes $Re_2X_4(\mu\text{-dppm})_2$ (X = Cl, Br; dppm = $Ph_2PCH_2PPh_2$) with Isocyanides. 18.[1] The Isolation and Characterization of Isomers of the $[Re_2Cl_2(\mu\text{-dppm})_2(CO)(CNXyl)_3]^{2+}$ Cation and Its Monocationic and Neutral Congeners

Yan Ding, Wengan Wu, Phillip E. Fanwick, and Richard A. Walton*

Department of Chemistry, Purdue University, 1393 Brown Building, West Lafayette, Indiana 47907-1393

Received October 7, 1998

The reactions of the multiply bonded dirhenium(II) complexes $Re_2Cl_4(\mu\text{-dppm})_2(CO)$, $Re_2Cl_4(\mu\text{-dppm})_2(CO)(CNXyl)$, and $[Re_2Cl_3(\mu\text{-dppm})_2(CO)(CNXyl)_2]O_3SCF_3$ (dppm = $Ph_2PCH_2PPh_2$; Xyl = 2,6-dimethylphenyl) with the requisite number of equivalents of TlO_3SCF_3 and XylNC lead to three, non-interconvertible, structural isomers of the complex $[Re_2Cl_2(\mu\text{-dppm})_2(CO)(CNXyl)_3](O_3SCF_3)_2$ (**4a**, **5a**, and **6a**; **a** signifies a triflate salt). Each of these complexes undergoes two reversible one-electron reductions which afford the redox pairs **4a′**/**4″**, **5a′**/**5″**, and **6a′**/**6″**, respectively. While **4a′** and **4″** have structures which are very similar to that of **4a**, the complexes **5a′**/**5″** and **6a′**/**6″** have structures which differ from **5a** and **6a**, thereby establishing the existence of coupled redox/isomerization reactions. Solutions of **6a′** in acetonitrile and **6″** in benzene slowly convert to the new isomers **7a′** and **8″**, respectively, which are in turn found to be members of the redox series **7′**/**7″** and **8**/**8′**/**8″**. In all, the $[Re_2Cl_2(\mu\text{-dppm})_2(CO)(CNXyl)_3]^{n+}$ species (n = 2, 1, or 0) have been found to exist in seven distinct structural forms which possess Re−Re bond orders of 3, 2, 1.5, 1, or 0 depending on the specific bioctahedral structure which is assumed and the charge on the complex. Single-crystal X-ray structure determinations have been carried out on the seven complexes **4″**, **5a**, **6a**, **6a′**, **6″**, **7a′**, and **7″**.

Introduction

Up to three π-acceptor ligands (designated L, L′ and L″) can be incorporated into the coordination sphere of the triply bonded dirhenium(II) synthons $Re_2X_4(\mu\text{-dppm})_2$ (X = Cl, Br; dppm = $Ph_2PCH_2PPh_2$)[2] as shown in the following sequence of reaction steps.

$$Re_2X_4(\mu\text{-dppm})_2 \xrightarrow{L} Re_2X_4(\mu\text{-dppm})_2L \xrightarrow{L'}$$

$$Re_2X_4(\mu\text{-dppm})_2LL' \xrightarrow[-X]{L''} [Re_2X_3(\mu\text{-dppm})_2LL'L'']^+$$

In the case of L = CO and L′ = L″ = XylNC (Xyl = 2,6-dimethylphenyl), a remarkable variety of structural isomers have been encountered with structures which are based upon open bioctahedral (**A**) and edge-sharing bioctahedral (**B**) geometries (L represents the halide, CO, or XylNC ligands)[1,3−11] with, in one instance, both boat and chair conformers for the $[Re_2(\mu\text{-dppm})_2]$ unit.[8,11]

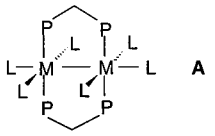

A

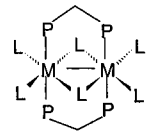

B

In the absence of bridging dppm ligands (and their like), reactions of dirhenium(II) compounds that contain the electron-rich triple bond ($\sigma^2\pi^4\delta^2\delta^{*2}$ electronic configuration)[2c] with π-acceptor ligands, especially CO and organic isocyanides, result in fragmentation to mononuclear species, as happens in the case of the triply bonded complexes $Re_2X_4(PR_3)_4$,[12,13] which contain monodentate rather than bridging bidentate phosphines. To establish the feasibility of increasing still further the number of π-acceptor ligands that can be bound to the $(Re{\equiv}Re)^{4+}$ core and ascertaining their influence upon the nature of the metal−metal bonding, we have developed strategies for the synthesis of salts of complex cations of the type $[Re_2Cl_2(\mu\text{-dppm})_2(CO)(CNXyl)_3]^{2+}$. This study constitutes the first in which four π-acceptors have been coordinated to the $(Re{\equiv}Re)^{4+}$ core, and the results demonstrate both the remarkable stability of the $[Re_2(\mu\text{-dppm})_2]^{4+}$ unit and the existence of a rich isomer chemistry for this new series of dirhenium complexes. The present report provides a detailed account of this chemistry, which has been the subject of two preliminary communications.[10,14]

(1) Part 17: Ding, Y.; Kort, D. A.; Wu, W.; Fanwick, P. E.; Walton, R. A. *J. Organomet. Chem.* **1999**, *573*, 87.
(2) (a) Price, A. C.; Walton, R. A. *Polyhedron* **1987**, *6*, 729. (b) Walton, R. A. *Polyhedron*, **1989**, *8*, 1689. (c) Cotton, F. A.; Walton, R. A. *Multiple Bonds between Metal Atoms*, 2nd ed.; Oxford University Press: Oxford, U.K., 1993.
(3) Anderson, L. B.; Cotton, F. A.; Dunbar, K. R.; Falvello, L. R.; Price, A. C.; Reid, A. H.; Walton, R. A. *Inorg. Chem.* **1987**, *26*, 2717.
(4) Wu, W.; Fanwick, P. E.; Walton, R. A. *Inorg. Chim. Acta* **1996**, *242*, 81.
(5) Wu, W.; Fanwick, P. E.; Walton, R. A. *J. Cluster Sci.* **1996**, *7*, 155.
(6) Wu, W.; Fanwick, P. E.; Walton, R. A. *Inorg. Chem.* **1996**, *35*, 5484.
(7) Wu, W.; Fanwick, P. E.; Walton, R. A. *J. Am. Chem. Soc.* **1996**, *118*, 13091.
(8) Wu, W.; Fanwick, P. E.; Walton, R. A. *J. Chem. Soc., Chem. Commun.* **1997**, 755.
(9) Wu, W.; Fanwick, P. E.; Walton, R. A. *Organometallics* **1997**, *16*, 1538.
(10) Wu, W.; Fanwick, P. E.; Walton, R. A. *J. Cluster Sci.* **1997**, *8*, 547.
(11) Wu, W.; Fanwick, P. E.; Walton, R. A. *Inorg. Chem.* **1998**, *37*, 3122.
(12) Walton, R. A. *ACS Symp. Ser.* **1981**, *155*, 207.
(13) Reference 2c, pp 114−115 and references therein.
(14) Wu, W.; Fanwick, P. E.; Walton, R. A. *Inorg. Chem.* **1997**, *36*, 3810.

10.1021/ic981192q CCC: $18.00
Published on Web 03/27/1999

Experimental Section

Starting Materials and General Procedures. The compounds $Re_2Cl_4(\mu\text{-dppm})_2(CO)$ (**1**),[15] $Re_2Cl_4(\mu\text{-dppm})_2(CO)(CNXyl)$ (**2**),[5] $[Re_2Cl_3(\mu\text{-dppm})_2(CO)(CNXyl)_2]O_3SCF_3$ (**3**),[5] $[Re_2Cl_3(\mu\text{-dppm})_2(CO)(CNXyl)]O_3SCF_3$,[16] TlO_3SCF_3,[17] and $[(\eta^5\text{-}C_5H_5)_2Fe]PF_6$[18] were prepared by standard literature procedures. Samples of 2,6-dimethylphenyl isocyanide (XylNC) were purchased from Fluka Chemical Corp., $TlPF_6$ and $NOPF_6$ from Strem Chemicals, and $(\eta^5\text{-}C_5H_5)_2Co$ from Aldrich Chemical Co. These commercial reagents were used as received. Solvents were obtained from commercial sources and were deoxygenated by purging with dinitrogen prior to use. All reactions were performed under an atmosphere of dinitrogen.

***CAUTION*:** Special precautions should be taken in handling thallium(I) compounds, which are toxic.

A. Synthesis of Isomers of $[Re_2Cl_2(\mu\text{-dppm})_2(CO)(CNXyl)_3](O_3SCF_3)_2$. (i) Isomer 4. (a) A mixture of $Re_2Cl_4(\mu\text{-dppm})_2(CO)$ (**1**) (50.0 mg, 0.038 mmol), XylNC (15.0 mg, 0.114 mmol), and TlO_3SCF_3 (27.0 mg, 0.076 mmol) was treated with 15 mL of dichloromethane and stirred at 25 °C for 8 h. The white precipitate of TlCl was filtered off, the red-brown filtrate reduced in volume to ca. 2 mL, and an excess of diethyl ether (25 mL) added to induce precipitation of **4a** as brown microcrystals; yield 62.5 mg (85%). Anal. Calcd for $C_{80}H_{71}Cl_2F_6N_3O_7P_4Re_2S_2$ (i.e., $[Re_2Cl_2(dppm)_2(CO)(CNXyl)_3](O_3SCF_3)_2$): C, 49.74; H, 3.70; N, 2.18. Found: C, 49.56; H, 3.65; N, 2.26. Conductivity measurement (in acetone): $\Lambda_m = 217\ \Omega^{-1}\ cm^2\ mol^{-1}$.

(b) A mixture of the complex $[Re_2Cl_3(\mu\text{-dppm})_2(CO)(CNXyl)]O_3SCF_3$ (150 mg, 0.0964 mmol) and 1 equiv of XylNC (12.6 mg, 0.096 mmol) was treated with 20 mL of dichloromethane and stirred at 25 °C for 20 h. The brown solution was reduced in volume to ca. 2 mL and 30 mL of diethyl ether added to induce precipitation of the complex $[Re_2Cl_3(\mu\text{-dppm})_2(CO)(CNXyl)_2]O_3SCF_3$, which is one of five known structural isomers of the $[Re_2Cl_3(\mu\text{-dppm})_2(CO)(CNXyl)_2]^+$ cation; yield 146.5 mg (90%). Anal. Calcd for $C_{72}H_{66}Cl_7F_3N_2O_4P_4Re_2S$ (i.e., $[Re_2Cl_3(dppm)_2(CO)(CNXyl)_2]O_3SCF_3\cdot 2CH_2Cl_2$): C, 46.57; H, 3.58; N, 1.51. Found: C, 46.39; H, 3.36; N, 1.63. Its spectroscopic properties and structural assignment have been reported previously,[10] while its cyclic voltammogram (in 0.1 M TBAH−CH_2Cl_2) is as follows: $E_{1/2}(ox) = +1.07$ V, $E_{1/2}(red) = -0.09$ V, and $E_{1/2}(red) = -0.89$ V vs Ag/AgCl. A portion of this product (80.0 mg, 0.0474 mmol) was then reacted with 1 equiv each of XylNC (6.2 mg, 0.0472 mmol) and TlO_3SCF_3 (16.7 mg, 0.0472 mmol) in 20 mL of dichloromethane at 25 °C for 16 h to afford brown microcrystals of **4a**; yield 80.0 mg (87%).

(c) The analogous $[PF_6]^-$ salt **4b** was obtained by a procedure very similar to that described in A(i)(a). The reaction of **1** (100 mg, 0.076 mmol) with 30.0 mg of XylNC (0.229 mmol) and 60.0 mg of $TlPF_6$ (0.160 mmol) in 18 mL of dichloromethane afforded $[Re_2Cl_2(\mu\text{-dppm})_2(CO)(CNXyl)_3](PF_6)_2$; yield 122 mg (83%). Its spectroscopic and electrochemical properties were essentially identical to those of the triflate salt **4a**.

(ii) Isomer 5. A quantity of the complex $Re_2Cl_4(\mu\text{-dppm})_2(CO)(CNXyl)$ (**2**) (100 mg, 0.0693 mmol) was mixed with 50.0 mg of TlO_3SCF_3 (0.141 mmol) and 18.5 mg of XylNC (0.147 mmol). This mixture was treated with 25 mL of dichloromethane at 25 °C and stirred for 12 h. A solid (TlCl) was filtered off, and the brown filtrate was reduced in volume to ca. 2 mL. An excess of diethyl ether (20 mL) was then added to the solution to induce precipitation. The title complex **5a** was collected by filtration; yield 130 mg (97%). Anal. Calcd for $C_{81}H_{73}Cl_4F_6N_3O_7P_4Re_2S_2$ (i.e., $[Re_2Cl_2(dppm)_2(CO)(CNXyl)_3](O_3SCF_3)_2\cdot CH_2Cl_2$): C, 48.21; H, 3.65; N, 2.08. Found: C, 48.25; H, 3.60; N, 2.05. Conductivity measurement (in acetone): $\Lambda_m = 216\ \Omega^{-1}\ cm^2\ mol^{-1}$.

(iii) Isomer 6. A mixture of the salt $[Re_2Cl_3(\mu\text{-dppm})_2(CO)(CNXyl)_2]O_3SCF_3$ (**3**) (45.0 mg, 0.027 mmol), TlO_3SCF_3 (9.5 mg, 0.027 mmol), and XylNC (3.5 mg, 0.027 mmol) in 15 mL of dichloromethane was stirred at 25 °C for 2 h. The precipitate of TlCl was filtered off, the volume of the red-brown filtrate was reduced to ca. 2 mL, and 15 mL of diethyl ether was then added to induce precipitation. The complex **6a** was harvested by filtration; yield 42.3 mg (80%). Anal. Calcd for $C_{80}H_{71}Cl_2F_6N_3O_7P_4Re_2S_2$ (i.e., $[Re_2Cl_2(dppm)_2(CO)(CNXyl)_3](O_3SCF_3)_2$): C, 49.74; H, 3.70; N, 2.18. Found: C, 49.45; H, 3.71; N, 2.37. Conductivity measurement (in acetone): $\Lambda_m = 218\ \Omega^{-1}\ cm^2\ mol^{-1}$.

B. Redox Reactions of Isomer 4. (i) Reduction to $[Re_2Cl_2(\mu\text{-dppm})_2(CO)(CNXyl)_3]O_3SCF_3$ (4a′). A mixture of **4a** (50.0 mg, 0.026 mmol) and $(\eta^5\text{-}C_5H_5)Co$ (5.0 mg, 0.026 mmol) was treated with 12 mL of dichloromethane at 25 °C, whereupon the color changed from red to green within 5 min. The resulting reaction mixture was stirred for 3 h and filtered, and an excess of diethyl ether was added to precipitate **4a′** as a green solid. This product was filtered off and dried; yield 46.0 mg (100%). Anal. Calcd for $C_{79}H_{71}Cl_2F_3N_3O_4P_4Re_2S$: C, 53.22; H, 4.02; N, 2.36. Found: C, 53.18; H, 3.97; N, 2.27. Conductivity measurement (in acetone): $\Lambda_m = 99\ \Omega^{-1}\ cm^2\ mol^{-1}$. When acetone was used as the reaction solvent in place of dichloromethane, the same product was obtained in almost quantitative yield.

Reduction of the analogous $[PF_6]^-$ salt **4b**, i.e., $[Re_2Cl_2(\mu\text{-dppm})_2(CO)(CNXyl)_3](PF_6)_2$, to the complex $[Re_2Cl_2(\mu\text{-dppm})_2(CO)(CNXyl)_3]PF_6$ (**4b′**) was accomplished upon its reaction with 1 equiv of $(\eta^5\text{-}C_5H_5)_2Co$. This product had the same CV properties as the triflate salt **4a′** and an IR spectrum very similar to that of **4a′**.

(ii) Reduction to $Re_2Cl_2(\mu\text{-dppm})_2(CO)(CNXyl)_3$ (4″). The use of a procedure similar to that described in B(i), but involving the reaction of **4a** with 2 equiv of $(\eta^5\text{-}C_5H_5)_2Co$, afforded the title complex **4″** in ca. 60% yield. Anal. Calcd for $C_{78}H_{71}Cl_2N_3OP_4Re_2$: C, 57.34; H, 4.38; N, 2.57. Found: C, 56.94; H, 4.27; N, 2.90. This same product was obtained by the reaction of 1 equiv of $(\eta^5\text{-}C_5H_5)_2Co$ with either **4a′** or **4b′**.

(iii) Oxidation of 4″ to 4b′. When a sample of **4″** was mixed with 1 equiv of $[(\eta^5\text{-}C_5H_5)_2Fe]PF_6$ in dichloromethane, a color change from red-brown to green occurred almost immediately. This mixture was stirred for 2 h and worked up in the usual way to afford $[Re_2Cl_2(\mu\text{-dppm})_2(CO)(CNXyl)_3]PF_6$ in essentially quantitative yield.

C. Redox Reactions of Isomer 5. (i) Reduction to $[Re_2Cl_2(\mu\text{-dppm})_2(CO)(CNXyl)_3]O_3SCF_3$ (5a′). A mixture of **5a** (50 mg, 0.026 mmol), $(\eta^5\text{-}C_5H_5)_2Co$ (5.0 mg, 0.026 mmol), and 5 mL of dichloromethane was stirred at 25 °C for 3 h, filtered, and evaporated to dryness with use of a rotary evaporator. The brown residue was washed with water and dried under a vacuum; yield 42.4 mg (92%). Anal. Calcd for $C_{79}H_{71}Cl_2F_3N_3O_4P_4Re_2S$: C, 53.22; H, 4.01. Found: C, 52.78; H, 3.62. Conductivity measurement (in acetone): $\Lambda_m = 138\ \Omega^{-1}\ cm^2\ mol^{-1}$.

(ii) Reduction to $Re_2Cl_2(\mu\text{-dppm})_2(CO)(CNXyl)_3$ (5″). The reaction between **5a** (50 mg, 0.026 mmol) and $(\eta^5\text{-}C_5H_5)_2Co$ (10.0 mg, 0.053 mmol) was carried out as described in C(i), the filtrate evaporated to dryness, and the residue extracted with benzene (20 mL). The extract was filtered, the filtrate evaporated to dryness, and the brown solid dried under a vacuum; yield 34.1 mg (81%). Anal. Calcd for $C_{78}H_{71}Cl_2N_3OP_4Re$: C, 57.35; H, 4.38. Found: C, 56.91; H, 4.39.

(iii) Oxidation of 5a′ to $[Re_2Cl_2(\mu\text{-dppm})_2(CO)(CNXyl)_3](O_5SCF_3)(PF_6)$. A mixture of **5a′** (75.2 mg, 0.042 mmol) and $NOPF_6$ (8 mg, 0.046 mmol) in 5 mL of dichloromethane was stirred for 1 h at 25 °C and filtered, and the volume of the filtrate was reduced to ca. 2 mL by use of a rotary evaporator. Diethyl ether (20 mL) was added to precipitate a brown solid, which was filtered off, washed with diethyl ether (2 × 5 mL), and dried under a vacuum; yield 60.2 mg (74%). The spectroscopic and electrochemical properties of the product are identical to those of compound **5** except for the presence of an IR band at 840 cm^{-1} due to the $[PF_6]^-$ anion.

(iv) Oxidation of 5″ to 5b′. The reaction between **5″** (50.0 mg, 0.0306 mmol) and $[(\eta^5\text{-}C_5H_5)_2Fe]PF_6$ (10.1 mg, 0.0305 mmol) in 5 mL of dichloromethane was carried out at 25 °C for 2 h with continuous stirring. The mixture was filtered, the filtrate reduced in volume to ca.

(15) Cotton, F. A.; Daniels, L. M.; Dunbar, K. R.; Falvello, L. R.; Tetrick, S. M.; Walton, R. A. *J. Am. Chem. Soc.* **1985**, *107*, 3524.
(16) Wu, W.; Subramony, J. A.; Fanwick, P. E.; Walton, R. A. *Inorg. Chem.* **1996**, *35*, 6784.
(17) Woodhouse, M. E.; Lewis, F. D.; Marks, T. J. *J. Am. Chem. Soc.* **1982**, *104*, 5586.
(18) Hendrickson, D. N.; Sohn, Y. S.; Gray, H. B. *Inorg. Chem.* **1971**, *10*, 1560.

1 mL under a stream of dinitrogen, and diethyl ether (20 mL) added to precipitate a brown solid. The solid was filtered off, washed with diethyl ether (2 × 5 mL), and dried under a vacuum; yield 39.2 mg (72%). The spectroscopic and electrochemical properties of this product are identical to those of **5a′** except for the presence of IR bands due to the $[PF_6]^-$ anion in place of those due to triflate.

D. Redox Reactions of Isomer 6. (i) Reduction to $[Re_2Cl_2(\mu\text{-dppm})_2(CO)(CNXyl)_3]O_3SCF_3$ (6a′). A procedure similar to that described in C(i) was used to prepare **6a′** as a green solid; yield 93%. Anal. Calcd for $C_{79}H_{71}Cl_2F_3N_3O_4P_4Re_2S$: C, 53.22; H, 4.01. Found: C, 52.87; H, 3.85. Conductivity measurement (in acetone): $\Lambda_m = 119\ \Omega^{-1}\ cm^2\ mol^{-1}$.

(ii) Reduction to $Re_2Cl_2(\mu\text{-dppm})_2(CO)(CNXyl)_3$ (6″). A procedure similar to that described in C(ii) was used to prepare **6″** as a brown solid; yield 72%. Anal. Calcd for $C_{78}H_{71}Cl_2N_3OP_4Re$: C, 57.35; H, 4.38. Found: C, 57.41; H, 4.30.

(iii) Oxidation of 6″ to 6b′. This green-colored title complex was prepared from the reaction of **6″** with $[(\eta^5\text{-}C_5H_5)_2Fe]PF_6$ by the use of a procedure similar to that described in C(iii); yield 57%. The spectroscopic and electrochemical properties of this product are identical to those of **6a′** except for IR bands due to the presence of $[PF_6]^-$ and absence of triflate.

(iv) Oxidation of 6a′ to $[Re_2Cl_2(\mu\text{-dppm})_2(CO)(CNXyl)_3](O_3SCF_3)(PF_6)$. The oxidation of **6a′** with the use of $[(\eta^5\text{-}C_5H_5)_2Fe]PF_6$ was carried out as described in C(iii) to afford the title complex; yield 58%. The spectroscopic and electrochemical properties of this product are the same as those of **6a** with the exception that its IR spectrum shows bands characteristic of the presence of both the $[PF_6]^-$ (840 cm^{-1}) and triflate (1260 cm^{-1}) anions.

E. Isomerization of 6a′ to 7a′. A quantity of **6a′** (50.0 mg, 0.0280 mmol) was dissolved in acetonitrile (10 mL) and the solution set aside for 3 days at 25 °C. During this time the color changed from green to purple. The solvent was removed by use of a rotary evaporator. The residue was recrystallized from dichloromethane/diethyl ether; yield 39.0 mg (78%). Anal. Calcd for $C_{79}H_{71}Cl_2F_3N_3O_4P_4Re_2S$: C, 53.22; H, 4.01. Found: C, 52.36; H, 4.01. Conductivity measurement (in acetone): $\Lambda_m = 126\ \Omega^{-1}\ cm^2\ mol^{-1}$.

F. Redox Reactions of 7a′. (i) Reduction to $Re_2Cl_2(\mu\text{-dppm})_2(CO)(CNXyl)_3$ (7″). An equimolar mixture of **7a′** (30.6 mg, 0.0172 mmol) and $(\eta^5\text{-}C_5H_5)_2Co$ (3.2 mg, 0.017 mmol) was dissolved in 5 mL of dichloromethane and stirred for 2 h, during which time the color changed from purple to yellow-green. The solvent was removed by use of a rotatory evaporator, the residue extracted with benzene (10 mL), the extract filtered, and the solvent evaporated to afford a green solid; yield 17.7 mg (63%). Anal. Calcd for $C_{78}H_{71}Cl_2N_3OP_4Re_2$: C, 57.35; H, 4.38. Found: C, 57.03; H, 4.13.

(ii) Oxidation of 7″ to 7b′. The complex **7″** was reoxidized to **7b′** through the use of $[(\eta^5\text{-}C_5H_5)_2Fe]PF_6$ as the oxidant and a procedure similar to that described in C(iii); yield 68%. The spectroscopic and electrochemical properties of this product were the same as those of **7a′** with the exception of the presence of IR bands due to the $[PF_6]^-$ anion in place of those due to triflate.

(iii) Attempted Oxidation of 7a′ to $[Re_2Cl_2(\mu\text{-dppm})_2(CO)(CNXyl)_3](O_3SCF_3)(PF_6)$. Attempts to oxidize **7a′** to the title complex through the use of a stoichiometric amount of $NOPF_6$ in dichloromethane were unsuccessful. The starting material was recovered unchanged.

G. Isomerization of 6″ to 8″. A solution of **6″** (100 mg, 0.0612 mmol) in benzene (10 mL) was set aside and the solvent allowed to slowly evaporate over a period of 2 weeks. This afforded a mixture of a yellow powder and a few green crystals, the latter being identified by IR spectroscopy as the perrhenate salt of the monocation which is present in **6a′** and **6b′** (ν(Re−O) at 910 (s) cm^{-1}). The yellow solid was extracted into 10 mL of benzene, the extract filtered, and the solvent evaporated to afford a yellow microcrystalline solid; yield 71.2 mg (71%). Anal. Calcd for $C_{78}H_{71}Cl_2N_3OP_4Re_2$: C, 57.35; H, 4.38. Found: C, 57.94; H, 4.56.

H. Redox Reactions of 8″. (i) Oxidation to 8b′. A mixture of **8″** (65.0 mg, 0.0398 mmol) and $[(\eta^5\text{-}C_5H_5)_2Fe]PF_6$ (13.2 mg, 0.0399 mmol) in 5 mL of dichloromethane was stirred at 25 °C for 3 h, during which time its color changed from yellow to green. The volume of the solution was reduced to ca. 1 mL, and 20 mL of benzene was added to precipitate a green solid. The mixture was filtered and the green product washed with benzene (2 × 5 mL) and dried under a vacuum; yield 57.3 mg (81%). Anal. Calcd for $C_{78}H_{71}Cl_2F_6N_3OP_5Re$: C, 52.67; H, 4.02. Found: C, 52.94; H, 4.57.

(ii) Oxidation to 8b. A quantity of **8″** (52.3 mg, 0.0320 mmol) was mixed with 2 equiv of $NOPF_6$ (11.2 mg, 0.0640 mmol) in 5 mL of dichloromethane, whereupon the color of the mixture turned from yellow to red. The mixture was stirred at 25 °C for 1 h and an excess of diethyl ether (15 mL) added to precipitate a red solid. This product was filtered off, washed with diethyl ether (2 × 5 mL), and dried under a vacuum; yield 33.1 mg (54%). Anal. Calcd for $C_{78}H_{71}Cl_2F_{12}N_3OP_6Re_2$: C, 48.70; H, 3.72. Found: C, 48.47; H, 3.78.

(iii) Reduction of 8b to 8b′. A mixture of **8b** (51.0 mg, 0.0265 mmol) and $(\eta^5\text{-}C_5H_5)_2Co$ (5.0 mg, 0.0264 mmol) in 5 mL of dichloromethane was stirred for 2 h and then filtered, and the filtrate was layered with 30 mL of diethyl ether. The green product **8b′** was collected by filtration, washed with water (10 mL) and diethyl ether (2 × 5 mL), and dried under a vacuum; yield 39.6 mg (84%).

(iv) Reduction of 8b′ to 8″. An equimolar mixture of **8b′** (35.1 mg, 0.0197 mmol) and $(\eta^5\text{-}C_5H_5)_2Co$ (3.7 mg, 0.0196 mmol) in 5 mL of dichloromethane was stirred at 25 °C for 2 h. The reaction mixture changed color from green to yellow during this period. The solvent was removed by use of a rotary evaporator, the residue was extracted with benzene (10 mL), and the extract was evaporated to dryness to yield the yellow compound **8″**, yield 24.4 mg (76%).

X-ray Crystallography. Single crystals of **4″**, **5a**, and **6a** were grown at 25 °C by slow evaporation of the solvents (**4″** from C_6H_6/*n*-C_7H_{16} (2:1), **5a** from CH_2Cl_2/*i*-Pr_2O (2:1), and **6a** from $C_2H_4Cl_2/C_6H_5(CH_3)$ (2:1)) while single crystals of **6a′**, **6″**, **7a′**, and **7″** were grown by slow diffusion of diethyl ether into dichloromethane solutions of the complexes. The crystals were mounted on glass fibers in random orientations. The data collections for **4″**, **5a**, **6a**, **6a′**, **7a′**, and **7″** were performed on an Enraf-Nonius CAD4 diffractometer equipped with a graphite monochromator, and that for **6″** was performed on a Nonius KappaCCD diffractometer. Data were collected at 295 ± 1 K for **5a**, **6a**, **6″**, **7a′**, and **7″**, and at 203 ± 1 K for **4″** and **6a′**. The crystallographic data for the compounds are given in Table 1.

The positions of the Re atoms were determined from Patterson maps; other non-hydrogen atoms were located in difference Fourier syntheses. In the case of structures **4″**, **5a**, **6a**, and **6a′**, hydrogen atoms were placed in calculated positions according to idealized geometries with C−H = 0.95 Å and $U(H) = 1.3U_{eq}(C)$. They were included in the refinement but constrained to ride on the atom to which they are bonded. Hydrogen atoms were not included in the structure analyses of **6″**, **7a′**, and **7″**. Empirical absorption corrections were applied in all cases except for the structure of **6″**; for **4″** the method of Parkin et al.[21] was applied, while that of Walker and Stuart[22] was used for **5a**, **6a**, **6a′**, **7a′**, and **7″**. All of the calculations were performed on a VAX computer (**4″**, **5a**, and **6a**) or an AlphaServer 2100 computer (**6a′**, **6″**, **7a′**, and **7″**). The final refinements were performed by the use of the programs SHELXL-93[19] (**4″**, **5a**, and **6a**) and SHELXL-97[20] (**6a′**, **6″**, **7a′**, and **7″**). All structures were refined in full-matrix least squares where the function minimized was $\sum w(|F_o|^2 - |F_c|^2)^2$.

All non-hydrogen atoms in **4″** were refined with anisotropic thermal parameters. Three benzene molecules from the crystallization solvents were found cocrystallized with **4″** in the asymmetric unit during the course of the structure analysis. They were included in the analysis and refined satisfactorily. The largest remaining peak in the final difference Fourier was 1.77 e/Å^3.

All non-hydrogen atoms in **5a** were refined with anisotropic thermal parameters. Two sites of partial molecules of CH_2Cl_2 from the

(19) Sheldrick, G. M. *SHELXL-93. A Program for Crystal Structure Refinement*; University of Göttingen: Göttingen, Germany, 1993.
(20) Sheldrick, G. M. *SHELXL-97. A Program for Crystal Structure Refinement*; University of Göttingen: Göttingen, Germany, 1997.
(21) Parkin, S.; Moezzi, B.; Hope, H. *J. Appl. Crystallogr.* **1995**, *28*, 53.
(22) Walker, N.; Stuart, D. *Acta Crystallogr., Sect. A* **1983**, *39*, 158.

Table 1. Crystallographic Data for the Dirhenium Complexes of the Type $[Re_2Cl_2(\mu\text{-dppm})_2(CO)(CNXyl)_3]^{n+}$, ($n$ = 2, 1, or 0)

	4″	**5a**	**6a**	**6a′**	**6″**	**7a′**	**7″**
empirical formula	$Re_2Cl_2P_4ON_3C_{96}H_{89}$	$Re_2Cl_{5.48}S_2P_4F_6O_7N_3C_{81.74}H_{74}$	$Re_2Cl_{5.25}S_{1.75}P_4F_{5.25}O_{6.25}N_3C_{89.75}H_{85}$	$Re_2Cl_6SP_4F_3O_4N_3C_{81}H_{75}$	$Re_2Cl_2P_4ON_3C_{78}H_{71}$	$Re_2Cl_2SP_4F_3O_4N_3C_{79}H_{71}$	$Re_2Cl_2P_4ON_3C_{78}H_{71}$
fw	1868.00	2709.66	2143.86	1952.59	1633.66	1782.72	1633.66
space group	$P2_1/n$ (No. 14)	$P2_1/n$ (No. 14)	$P2_1/c$ (No. 14)	$P2_1/n$ (No. 14)	$P\bar{1}$ (No. 2)	$P\bar{1}$ (No. 2)	$P\bar{1}$ (No. 2)
a, Å	15.003(2)	23.582(5)	22.642(5)	15.663(4)	15.1232(5)	14.070(3)	15.095 (5)
b, Å	33.588(13)	16.344(6)	13.960(5)	23.826(6)	23.6696(8)	15.680(4)	18.838 (4)
c, Å	16.215(5)	23.656(6)	32.725(15)	22.492(6)	24.4036(8)	20.542(5)	21.811 (6)
α, deg					111.2994(19)	76.73(2)	68.21 (7)
β, deg	92.031(16)	109.091(18)	109.65(3)	107.26(2)	96.439(2)	75.93(2)	77.31 (5)
γ, deg					104.598(2)	87.935(18)	85.31 (5)
V, Å^3	8166(7)	8616(8)	9741(11)	8015(7)	7672.4(11)	4277(2)	5618(6)
Z	4	4	4	4	4	2	3
ρ_{calcd}, g/cm^3	1.519	1.603	1.462	1.618	1.414	1.384	1.448
μ, mm^{-1}	3.194	3.208	2.827	3.420	3.389	7.187	3.471
radiation (λ, Å)	Mo Kα (0.710 73)	Mo Kα (0.710 73)	Mo Kα (0.710 73)	Mo Kα (0.710 73)	Mo Kα (0.710 73)	Cu Kα (1.541 84)	Mo Kα (0.710 73)
trans factors, min/max	0.33, 0.54	0.19, 0.29	0.59, 0.90	0.23, 0.43		0.22, 0.56	0.10, 0.18
temp, K	203	295	295	203	296	296	296
$R(F_o)^a$	0.034	0.047	0.045	0.037	0.081	0.105	0.050
$R_w(F_o^2)^b$	0.082	0.114	0.128	0.090	0.213	0.214	0.126
GOF	1.042	1.052	1.107	1.049	0.891	1.106	1.099

[a] $R = \sum||F_o| - |F_c||/\sum|F_o|$. [b] $R_w = [\sum w(|F_o^2| - |F_c^2|)^2/\sum w(|F_o^2|)^2]^{1/2}$.

crystallization solvent were found in the asymmetric unit; their C and Cl atoms were located and refined satisfactorily with anisotropic thermal parameters. Refinement of these two solvent molecules gave occupancies of 0.906 and 0.835. The largest remaining peak in the final difference Fourier was 1.59 e/Å^3.

During the course of the structure analysis of **6a**, one of the two $[CF_3SO_3]^-$ anions was found to be disordered with a Cl^- anion. This disordered model was included in the analysis, and these two disordered anionic groups were refined to occupancies of 0.749 for $[CF_3SO_3]^-$ and 0.251 for Cl^-. Several molecules from the crystallization solvents were also found in the asymmetric unit. These consisted of one full site and one partially occupied site (fixed to an occupancy of 0.500) of 1,2-dichloroethane, and one full site of toluene. These molecules were included in the analysis and satisfactorily refined. During the final stage of the analysis, two carbon atoms, C(200) and C(812), which belong to the disordered triflate anion and the one-half molecule of $C_2H_4Cl_2$, respectively, did not refine to convergence; they were included with rigid positional parameters in the final refinement. All other non-hydrogen atoms were refined with anisotropic thermal parameters. The largest remaining peak in the final difference Fourier was 2.00 e/Å^3.

For **6a′**, it was found that the CO ligand was disordered with the terminal chlorine atom. This disorder is generated by a pseudotwofold axis through the bridging chlorine atom Cl(12) and the carbon atom C(30) of the bridging xylyl isocyanide ligand. Two different sets of positions were produced and refined satisfactorily to a 0.73/0.27 disorder model. Two CH_2Cl_2 solvent molecules were also found in the asymmetric unit. They were included in the analysis and satisfactorily refined. All of the non-hydrogen atoms were refined with anisotropic thermal parameters except for the disordered CO ligand. The largest remaining peak in the final difference Fourier was 1.19 e/Å^3.

There are two independent molecules of **6″** in the asymmetric unit. A disordered solvent molecule was removed with the squeeze option in PLATON.[23] Atoms N(30), N(50), and C(50) were refined with isotropic thermal parameters, and all other non-hydrogen atoms were refined with anisotropic thermal parameters. The largest remaining peak in the final difference Fourier was 1.98 e/Å^3.

The $[CF_3SO_3]^-$ anion of **7a′** was disordered so badly that the squeeze option in PLATON[23] was used to remove the anion. All non-hydrogen atoms of the cation were refined with anisotropic thermal parameters except for one carbon atom, C(30), which was refined isotropically. The largest remaining peak in the final difference Fourier was 1.82 e/Å^3.

There are one and one-half independent molecules of **7″** in the asymmetric unit. A disorder involving the terminal CO and xylyl isocyanide ligands occurs for the half-molecule which is located about the inversion center. In this disorder model the C and O atoms of the CO ligand were indistinguishable from the C and N atoms of the XylNC ligands. Also, there are two sites (50:50 occupancy) of partial xylyl groups for each of the three disordered xylyl isocyanide ligands. Accordingly, each partial xylyl group was refined to an occupancy of 0.375 (i.e., 0.75 × 0.50). All non-hydrogen atoms were refined with anisotropic thermal parameters except for a carbon atom of one of the isocyanide ligands, C(37), and those carbon atoms of the disordered xylyl fragments which were refined isotropically. The largest remaining peak in the final difference Fourier was 1.82 e/Å^3.

Physical Measurements. Routine IR spectra, ^{1}H and ^{31}P{^{1}H} NMR spectra, and cyclic voltammetric (CV) measurements were determined as described previously.[24] Variable temperature ^{31}P{^{1}H} NMR spectra were obtained on a Varian XL-200 spectrometer operated at 80.98 MHz. The solid state ^{31}P{^{1}H} NMR spectrum of **5a** was recorded on a Bruker AC-250 NMR spectrometer equipped with a CP/MAS broad-band VT probe operated at 101.3 MHz; the spectrum was referenced to $Na_2H_2P_2O_7$ ($\delta = -13.0$). Elemental microanalyses were carried out by Dr. H. D. Lee of the Purdue University Microanalytical Laboratory.

Results and Discussion

The feasibility of coordinating four π-acceptor ligands (three XylNC ligands and one CO ligand) is demonstrated in Scheme 1, where each of the starting materials **1**, **2**, and **3** is seen to convert to an isomer of the $[Re_2Cl_2(\mu\text{-dppm})_2(CO)(CNXyl)_3]^{2+}$ cation (**4**, **5**, and **6**) upon reaction with the requisite number of equivalents of Tl^+ (as its $[O_3SCF_3]^-$ or $[PF_6]^-$ salts) and XylNC. Note that, under the conditions used to convert **2** to **5**, compound **3** is not a reaction intermediate. In all subsequent discussions, the designations **a** and **b** will be used for the triflate and hexafluorophosphate salts, respectively, of the dications **4**−**6** and their monocationic analogues. Most studies were conducted on the triflate salts; in those cases where the $[PF_6]^-$ salts were isolated, their spectroscopic and electrochemical properties were found to be essentially identical to those of their triflate analogues.

Despite our earlier work[5] which established the synthetic procedures by which complex **1** can be converted sequentially

(23) Sluis, P. V. D.; Spek, A. L. *Acta Crystallogr., Sect. A* **1990**, *46*, 194.

(24) Wu, W.; Fanwick, P. E.; Walton, R. A. *Inorg. Chem.* **1995**, *34*, 5810.

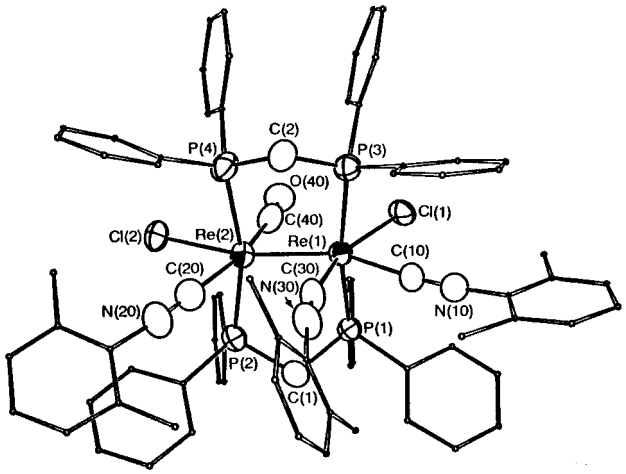

Figure 1. ORTEP[25] representation of the structure of the dirhenium cation $[Re_2Cl_2(\mu\text{-dppm})_2(CO)(CNXyl)_3]^{2+}$ as present in **5a**. The thermal ellipsoids are drawn at the 50% probability level, except for the phenyl group atoms of the dppm ligands and the xylyl group atoms of the XylNC ligands, which are circles of arbitrary radius.

Scheme 1. Isomers **4**−**6** of the Dirhenium Cation $[Re_2Cl_2(\mu\text{-dppm})_2(CO)(CNXyl)_3]^{2+}$ (R = Xyl)

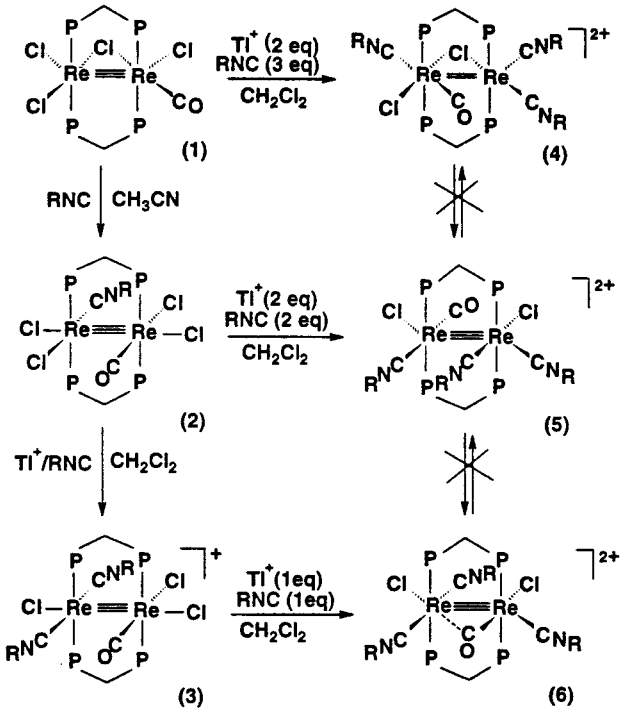

to **2** and then to **3**, the three isomeric forms of $[Re_2Cl_2(\mu\text{-dppm})_2(CO)(CNXyl)_3]^{2+}$ (**4**−**6**), which are formed from **1**−**3**, are kinetically stable and show no tendency to interconvert under thermal conditions. This has enabled us to fully characterize these complexes by a combination of IR and NMR spectroscopy, cyclic voltammetry (CV), and X-ray crystallography. The isomeric forms **4a**, **5a**, and **6a** of $[Re_2Cl_2(\mu\text{-dppm})_2(CO)(CNXyl)_3](O_3SCF_3)_2$ are easily distinguished by a combination of the spectroscopic and electrochemical data shown in Tables 2 and 3. In all three cases, the ν(CO) mode is assigned to the lowest of the frequencies in the region 2200−1800 cm^{-1}. The $^{31}P\{^1H\}$ NMR spectra are quite simple; **4a** shows the expected AA′BB′ pattern, but for **5a** and **6a** the spectra consist of a singlet which is most readily explained in terms of fluxional behavior (vide infra).

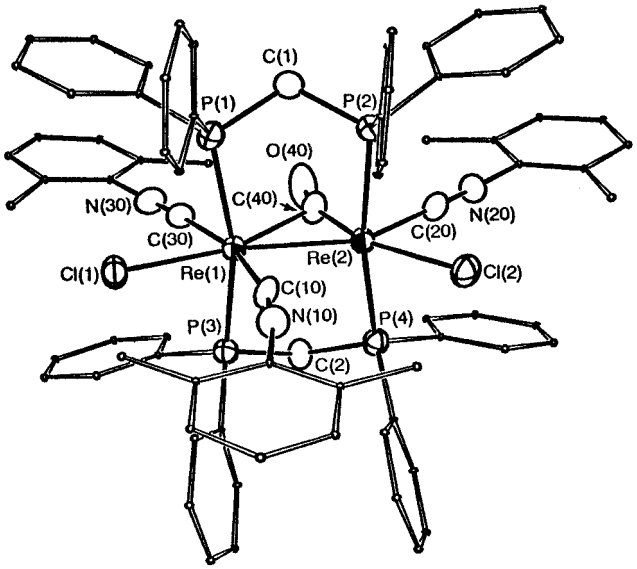

Figure 2. ORTEP[25] representation of the structure of the dirhenium cation $[Re_2Cl_2(\mu\text{-dppm})_2(CO)(CNXyl)_3]^{2+}$ as present in **6a**. The thermal ellipsoids are drawn at the 50% probability level, except for the phenyl group atoms of the dppm ligands and the xylyl group atoms of the XylNC ligands, which are circles of arbitrary radius.

For all three complexes, attempts were made to obtain single crystals for X-ray diffraction analysis. We were successful in the case of **5a** and **6a**, and the ORTEP[25] representations of the dirhenium cations present in the structures are shown in Figures 1 and 2. Important structural parameters are given in Table 4. Bond angle data between the axial P atoms of the dppm ligands and the ligand atoms in the equatorial plane are not listed but are available in the Supporting Information. The Re−Re bond lengths for the dirhenium cations of **5a** and **6a** of 2.4728(7) and 2.4968(8) Å, respectively, are consistent with the presence of Re≡Re bonds which have been weakened by π-back-bonding from the Re_2 core to the XylNC(π*) and CO(π*) ligand orbitals. The persistence of a triple bond would also be in accord with an 18-electron count for the Re centers in these $[Re_2Cl_2(\mu\text{-dppm})_2(CO)(CNXyl)_3]^{2+}$ cations.

Of the three XylNC ligands of **5a**, the one bound to Re(1) shows the smallest Re−C−N angle (N(30)−C(30)−Re(1) = 165.5(8) Å). However, there is no indication of a significant bridging interaction between this ligand and Re(2) since the distance Re(2)−C(30) is 2.600(9) Å; the corresponding nonbonding distance involving the carbonyl carbon atom C(40) (i.e., Re(1)−C(40)) is 2.610(10) Å. In contrast, there is a clear indication of a weak unsymmetrical CO bridge in **6a**, with Re−C distances of 1.894(7) Å for Re(2)−C(40) and 2.381(8) Å for Re(1)−C(40). The carbon atom C(10) of the XylNC ligand most able to form a bridge is at a nonbonding distance to Re(2) (i.e., ca. 2.78 Å), so the solid state structure of **6a** is quite unsymmetrical. Nonetheless, this structure gives a clue as to the explanation for the simplicity of the room temperature $^{31}P\{^1H\}$ NMR spectra of **6a** and **5a** (see Table 2), namely, fluxional processes where the two halves of the molecules are rendered equivalent through the intermediacy of symmetrical CO and XylNC ligand-bridged structures of the type $[(XylNC)ClRe(\mu\text{-CO})(\mu\text{-CNXyl})(\mu\text{-dppm})_2ReCl(CNXyl)]^{2+}$. This type of "windshield wiper" mechanism, involving a symmetrical edge-sharing

(25) (a) Johnson, C. K. ORTEP II. Report ORNL-5138; Oak Ridge National Laboratory: Oak Ridge, TN, 1976. (b) Farrugia, L. J. *J. Appl. Crystallogr.* **1997**, 565.

Table 2. Selected IR and NMR Spectral Data for the Various Isomers of the Dirhenium Complexes $[Re_2Cl_2(\mu\text{-dppm})_2(CO)(CNXyl)_3]A_n$ (n = 2, 1 or 0)

complex			IR, cm^{-1} [a]	chem shift, δ[b]	
no.	A	n	ν(CN) and ν(CO)	$^{31}P\{^1H\}$ NMR	^1H NMR
4a	O_3SCF_3	2	2188 (m), 2126 (s), 2096 (s, br), *1800 (m−s)*	−9.8 (m),[c] −26.2 (m)[c]	+5.79 (m, 2H), +5.45 (m, 2H) [$-CH_2-$ of dppm], +2.66 (s, 6H), +2.24 (s, br, 12H) [CH_3 of Xyl]
4a′	O_3SCF_3	1	2160 (m−s), 2060 (s), 1994 (s, br), *1798 (m)*	*e*	*e*
4′		0	2124 (s), 2000 (vs, br), ∼1900 (vs, br), *1800 (m)*	+6.4 (m),[c] −13.0 (m)[c]	+3.80 (m, br, 2H), +2.40 (m, br, 2H) [$-CH_2-$ of dppm], +2.64 (s, 6H), +1.97 (s, 6H), +1.92 (s, 6H) [CH_3 of Xyl]
5a	O_3SCF_3	2	2162 (m), 2030 (m), 1996 (sh), *1936 (s)*	−17.9 (s)	+6.54 (m, 2H), +5.50 (m, 2H) [$-CH_2-$ of dppm], +3.07 (s, 6H), +1.35 (s, 12H) [CH_3 of Xyl]
5a′	O_3SCF_3	1	2091 (s), 2046 (s), 2007 (sh), 1976 (vs), 1853 (vs)	*e*	*e*
5″		0	2087 (m−w), 1998 (s), 1956 (s), 1902 (vs, br), 1856 (sh), 1787 (sh)	+10.3 (s),[c] +9.5 (s)[c]	+4.67 (m, 2H), +4.20 (m, 2H) [$-CH_2-$ of dppm], +1.81 (s, 6H), +1.75 (s, 6H), +1.71 (s, 6H) [CH_3 of Xyl]
6a	O_3SCF_3	2	2196 (m), 2166 (vs), 2056 (vs), *1964 (s, br)*	−7.6 (s)	+5.70(m,4H) [$-CH_2-$ of dppm], +3.13(s,6H), ∼+1.9 (s, vbr, 12H) [CH_3 of Xyl]
6a′	O_3SCF_3	1	2118 (m−s), 2049 (m−s), 2012 (m−w), 1945 (s, br), 1880 (m), 1869 (sh)	*e*	*e*
6″		0	2082 (s), 1978 (s), 1915 (vs, br), 1863 (sh)	+9.0 (m, br),[c] −6.3 (m, br)[c]	+3.98 (m, 2H), +3.54 (m, 2H) [$-CH_2-$ of dppm], +2.32 (s, 6H), +2.04 (s, 12H) [CH_3 of Xyl]
7a′	O_3SCF_3	1	2040 (sh), 2009 (vs), 1990 (sh), *1850 (vs)*	*e*	*e*
7″		0	2054 (m), 1981 (vs), *1842 (vs)*	+10.0 (s),[c] +9.1 (s)[c]	+4.62 (m, 2H), +4.27 (m, 2H) [$-CH_2-$ of dppm], +1.90 (s, 6H), +1.80 (s, 6H), +1.79 (s, 6H) [CH_3 of Xyl]
8b	PF_6	2	2160 (sh), 2149 (vs), 2119 (vs), *1737 (m)*	−14.8 (m),[c,d] −17.7 (m)[c,d]	+5.05 (m, 4H) [$-CH_2-$ of dppm], +2.55 (s, 12H), ∼+2.3 (br, 6H) [CH_3 of Xyl]
8b′	PF_6	1	2133 (s), 2074 (vs), 2038 (vs), 2020 (sh), 1992 (sh), *1747 (m)*	*e*	*e*
8″		0	2087 (vs), 2003 (vs), 1916 (vs, br), 1884 (sh), *1764 (m−s)*	+10.8 (m)[c], −1.2 (m)[c]	+4.07 (m, 2H), +3.46 (m, 2H) [$-CH_2-$ of dppm], +2.21 (s, 6H), +2.00 (s, 6H), +1.87 (s, 6H) [CH_3 of Xyl]

[a] IR spectra recorded as Nujol mulls. Bands assigned with confidence to ν(CO) modes are given in italics. Abbreviations: s = strong, m = medium, w = weak, br = broad, sh = shoulder. [b] NMR spectra recorded on CD_2Cl_2 solutions except for **4″**, whose spectra were recorded in C_6D_6, and **5″**, **6a**, and **6″**, whose spectra were recorded in $CDCl_3$. Abbreviations: s = singlet, m = multiplet, br = broad. [c] Components of an AA′BB′ splitting pattern. [d] The $^{31}P\{^1H\}$ NMR spectrum of **8b** also contains a heptet for the $[PF_6]^-$ anion at $\delta = -141.9$ (J_{P-F} = 711 Hz). [e] Paramagnetic. Broad, poorly defined ^1H NMR spectra except for **7a′**, which displayed a Knight shifted spectrum; no resonances seen in the $^{31}P\{^1H\}$ NMR spectra.

bioctahedral intermediate, is represented below for the dication **6**:

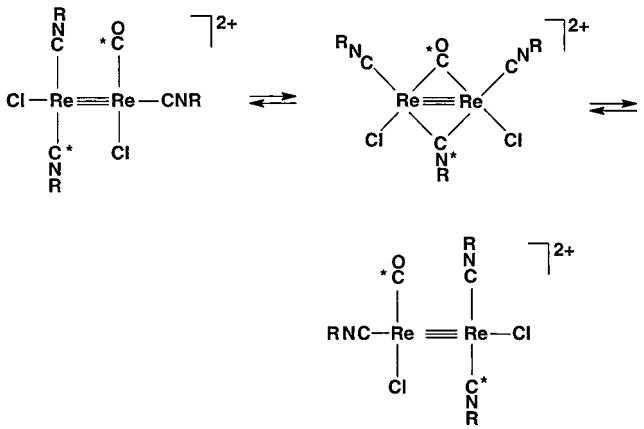

The structure of the cation **6** that is shown in Figure 2 can be considered to represent an intermediate stage in this process where the μ-CO and μ-CNXyl bridges are being formed or broken.

The $^{31}P\{^1H\}$ NMR spectra of solutions of **5a** and **6a** in CD_2Cl_2 were recorded over the temperature range +25 °C to −70 °C. Both spectra remained as sharp singlets over this range. The singlet at $\delta = -17.9$ in the spectrum of **5a** shifts to $\delta = -18.5$, while that at $\delta = -6.9$ in the spectrum of **6a** ($\delta = -7.6$ in $CDCl_3$) shifts slightly downfield to $\delta = -6.6$ by the time the low-temperature limit is reached. The ^1H NMR spectra of **5a** and **6a** changed little over this same temperature range, except for the very broad xylyl methyl resonance of **6a** at δ = ca. +1.9 (12H), which coalesced and split into singlets at δ =

Table 3. Electrochemical Properties for the Various Isomers of the Dirhenium Complexes $[Re_2Cl_2(\mu\text{-dppm})_2(CO)(CNXyl)_3]A_n$ (n = 2, 1, or 0)

complex			CV half-wave potentials, V[a]		
no.	A	n	$E_{p,a}$	$E_{p,c}$	$E_{1/2}$b
4a	O_3SCF_3	2			+0.50 (80),[d] −0.19 (80)[d]
4a′	O_3SCF_3	1			+0.51 (70),[c] −0.19 (70)[d]
4″		0			+0.49 (70),[c] −0.20 (75)[c]
5a	O_3SCF_3	2			+0.30 (80),[d] −0.43 (90)[d]
5a′	O_3SCF_3	1	+0.79	+0.21	−0.47 (70)[d]
5″		0	+0.79	+0.21	−0.47 (70)[c]
6a	O_3SCF_3	2			+0.26 (85),[d] −0.57 (85)[d]
6a′	O_3SCF_3	1	+0.57	+0.26	−0.24 (60)[c]
6″		0	+0.57	+0.26	−0.24 (60)[c]
7a′	O_3SCF_3	1			+1.34 (80),[c] +0.65 (70),[c] +0.18 (70)[d]
7″		0			+1.34 (80),[c] +0.65 (70),[c] +0.18 (70)[c]
8b	PF_6	2			+0.50 (60),[d] 0.00 (60)[d]
8b′	PF_6	1			+0.50 (60),[c] 0.00 (60)[d]
8″		0			+0.50 (60),[c] 0.00 (60)[c]

[a] Data are based upon single-scan cyclic voltammograms measured on 0.1 M TBAH/CH_2Cl_2 solutions and referenced to the Ag/AgCl electrode with a scan rate (ν) of 200 mV/s at a Pt-bead electrode. Under our experimental conditions, $E_{1/2}$ = +0.47 V for the ferrocenium/ferrocene couple. [b] $E_{1/2}$ values are for one-electron processes with $i_{p,a} = i_{p,c}$. Numbers in parentheses are the values of $E_{p,a} - E_{p,c}$ (in mV) for the process. [c] Oxidation for the bulk complex. [d] Reduction for the bulk complex.

Table 4. Key Bond Distances (Å) and Bond Angles (deg) for the Dirhenium Cations $[Re_2Cl_2(\mu\text{-dppm})_2(CO)(CNXyl)_3]^{2+}$ of **5a** and **6a** and the Molecule $Re_2Cl_2(\mu\text{-dppm})_2(CO)(CNXyl)_3$ of **4″** [a]

5a		**6a**		**4″**	
		Distances			
Re(1)−Re(2)	2.4728(7)	Re(1)−Re(2)	2.4968(8)	Re(1)−Re(2)	3.0442(7)
Re(1)−Cl(1)	2.433(2)	Re(1)−Cl(1)	2.436(2)	Re(1)−Cl(1)	2.4835(15)
Re(2)−Cl(2)	2.493(2)	Re(2)−Cl(2)	2.401(2)	Re(1)−Cl(12)	2.4843(15)
Re(1)−C(10)	2.063(9)	Re(1)−C(10)	2.044(7)	Re(2)−Cl(12)	2.511(2)
Re(1)−C(30)	2.008(10)	Re(1)−C(30)	2.078(7)	Re(1)−C(10)	2.049(6)
Re(2)−C(20)	2.145(12)	Re(2)−C(20)	2.048(8)	Re(2)−C(20)	1.897(6)
Re(1)−P(1)	2.491(2)	Re(1)−C(40)	2.381(8)	Re(2)−C(30)	1.912(6)
Re(1)−P(3)	2.492(2)	Re(2)−C(40)	1.894(7)	Re(1)−C(40)	1.980(6)
Re(2)−P(2)	2.500(3)	Re(1)−P(1)	2.491(2)	Re(1)−P(1)	2.3785(15)
Re(2)−P(4)	2.493(3)	Re(1)−P(3)	2.489(2)	Re(1)−P(3)	2.396(2)
Re(2)−C(40)	1.961(11)	Re(2)−P(2)	2.477(2)	Re(2)−P(2)	2.417(2)
C(10)−N(10)	1.154(11)	Re(2)−P(4)	2.474(2)	Re(2)−P(4)	2.405(2)
C(20)−N(20)	1.148(12)	C(10)−N(10)	1.164(9)	C(10)−N(10)	1.116(7)
C(30)−N(30)	1.133(11)	C(20)−N(20)	1.145(9)	C(20)−N(20)	1.206(7)
C(40)−O(40)	1.114(11)	C(30)−N(30)	1.136(9)	C(30)−N(30)	1.192(7)
		C(40)−O(40)	1.178(9)	C(40)−O(40)	1.127(7)
		Angles			
P(1)−Re(1)−P(3)	169.80(8)	P(1)−Re(1)−P(3)	165.26(6)	P(1)−Re(1)−P(3)	175.08(15)
C(30)−Re(1)−C(10)	77.6(4)	C(10)−Re(1)−C(30)	165.7(3)	C(40)−Re(1)−C(10)	164.5(2)
C(30)−Re(1)−Cl(1)	158.6(3)	C(10)−Re(1)−C(40)	120.5(3)	C(40)−Re(1)−Cl(1)	85.5(2)
C(10)−Re(1)−Cl(1)	81.0(3)	C(30)−Re(1)−C(40)	73.7(3)	C(10)−Re(1)−Cl(1)	79.1(2)
C(30)−Re(1)−Re(2)	70.1(3)	C(10)−Re(1)−Cl(1)	85.4(2)	C(40)−Re(1)−Cl(12)	111.2(2)
C(10)−Re(1)−Re(2)	47.7(2)	C(30)−Re(1)−Cl(1)	80.4(2)	C(10)−Re(1)−Cl(12)	84.3(2)
Cl(1)−Re(1)−Re(2)	131.28(6)	C(40)−Re(1)−Cl(1)	154.0(2)	Cl(1)−Re(1)−Cl(12)	163.36(5)
C(30)−Re(1)−C(40)	115.3(3)	C(10)−Re(1)−Re(2)	74.9(2)	C(40)−Re(1)−Re(2)	58.3(2)
C(10)−Re(1)−C(40)	166.8(3)	C(30)−Re(1)−Re(2)	119.3(2)	C(10)−Re(1)−Re(2)	137.1(2)
Cl(1)−Re(1)−C(40)	86.1(2)	C(40)−Re(1)−Re(2)	45.6(2)	Cl(1)− Re(1)−Re(2)	143.77(4)
Re(2)−Re(1)−C(40)	45.3(2)	Cl(1)−Re(1)−Re(2)	160.27(5)	Cl(12)−Re(1)−Re(2)	52.85(4)
P(2)−Re(2)−P(4)	165.00(8)	P(2)−Re(2)−P(4)	169.78(6)	P(2)−Re(2)−P(4)	172.98(5)
C(40)−Re(2)−C(20)	165.3(4)	C(40)−Re(2)−C(20)	76.3(3)	C(20)−Re(2)−C(30)	88.3(2)
C(40)−Re(2)−Re(1)	71.1(3)	C(40)−Re(2)−Cl(2)	157.5(2)	C(20)−Re(2)−Cl(12)	97.0(2)
C(20)−Re(2)−Re(1)	123.6(3)	C(20)−Re(2)−Cl(2)	81.2(2)	C(30)−Re(2)−Cl(12)	174.6(2)
C(40)−Re(2)−Cl(2)	84.6(3)	C(40)−Re(2)−Re(1)	64.0(2)	C(20)−Re(2)−C(40)	170.3(2)
C(20)−Re(2)−Cl(2)	80.7(3)	C(20)−Re(2)−Re(1)	140.2(2)	C(30)−Re(2)−C(40)	82.7(2)
Re(1)−Re(2)−Cl(2)	155.68(6)	Cl(2)−Re(2)−Re(1)	138.57(5)	Cl(12)−Re(2)−C(40)	92.10(14)
C(40)−Re(2)−C(30)	117.6(3)	N(10)−C(10)−Re(1)	168.0(6)	C(20)−Re(2)−Re(1)	149.0(2)
C(20)−Re(2)−C(30)	77.1(3)	N(20)−C(20)−Re(2)	178.0(6)	C(30)−Re(2)−Re(1)	122.7(2)
Re(1)−Re(2)−C(30)	46.5(2)	N(30)−C(30)−Re(1)	176.5(6)	Cl(12)−Re(2)−Re(1)	52.06(3)
Cl(2)- Re(2)−C(30)	157.7(2)	O(40)−C(40−Re(2)	161.0(6)	C(40)−Re(2)−Re(1)	40.05(14)
N(10)−C(10)−Re(1)	174.9(8)	O(40)−C(40)−Re(1)	128.5(6)	Re(1)−Cl(12)−Re(2)	75.09(4)
N(20)−C(20)−Re(2)	171.1(8)	Re(2)−C(40)−Re(1)	70.4(2)	N(10)−C(10)−Re(1)	178.8(5)
N(30)−C(30)−Re(1)	165.5(8)	C(10)−N(10)−C(11)	171.1(7)	N(20)−C(20)−Re(2)	176.8(5)
O(40)−C(40)−Re(2)	171.8(9)	C(20)−N(20)−C(21)	175.7(8)	N(30)−C(30)−Re(2)	177.0(5)
C(10)−N(10)−C(11)	175.4(10)	C(30)−N(30)−C(31)	174.2(8)	O(40)−C(40)−Re(1)	159.5(5)
C(20)−N(20)−C(21)	169.4(10)			Re(1)−C(40)−Re(2)	81.6(2)
C(30)−N(30)−C(31)	172.9(11)			C(10)−N(10)−C(11)	173.1(6)
				C(20)−N(20)−C(21)	161.4(6)
				C(30)−N(30)−C(31)	160.2(6)

[a] When appropriate, comparisons are made between corresponding parameters in the three structures as represented by the labeling schemes in Figures 1−3. Numbers in parentheses are estimated standard deviations in the least significant digits. Complete data are available as Supporting Information.

+2.67 (6H) and $\delta = +0.94$ (6H) as the temperature was lowered to ca. −70 °C. In contrast to the fluxional behavior which occurs in solution, the solid state $^{31}P\{^1H\}$ NMR spectrum of **5a** at +25 °C was found to consist of resonances at $\delta = -16.4$, −20.5, and −35.9 (intensity ratio of ca. 1:2:1). This spectrum changes very little upon warming the sample to +150 °C. Its complexity accords with the solid state structure as determined by X-ray crystallography (Figure 1) in which the four P atoms are magnetically inequivalent; the peak at $\delta = -20.5$ arises from the overlap of two of these resonances, while the other two are well resolved from one another.

Although the poor quality of the single crystals of **4a** precluded us from determining its X-ray crystal structure, the accessibility of its one- and two-electron-reduced congeners (**4a′** and **4″**) and the subsequent structure determination of **4″** enabled us to establish the structure of the salts of **4** and **4′**. The cyclic voltammetric properties of solutions of **4a** in 0.1 M TBAH/CH_2Cl_2 (see Table 3) consist of two reversible one-electron processes, corresponding to reductions of the bulk complex, at $E_{1/2} = +0.50$ V and $E_{1/2} = -0.19$ V vs Ag/AgCl. The processes can be accessed chemically through the use of cobaltocene as the reductant to afford the salt **4a′** and the neutral complex **4″**. The reoxidation of **4″** to the $[PF_6]^-$ salt **4b′** can be accomplished through the use of $[(\eta^5\text{-}C_5H_5)_2Fe]PF_6$. This chemistry is represented in Scheme 2. On the basis of the reversibility of the electrochemical properties of these complexes (Table 3), a comparison of their spectroscopic properties (Table 2), and a single-crystal X-ray structure determination of **4″**, we conclude that these three species have very similar structures as we have represented in Scheme 2. The structure of **4″** (Figure 3) shows the presence of a fairly symmetrical chloro bridge. The large disparity between the distances Re(1)−C(40) and Re(2)−C(40), which are 1.980(6) and 2.619(5) Å, respectively, along with an angle of 159.5(5)° for O(40)−C(40)−Re(1), indicates that the CO ligand forms at most a very weak bridge. The N−C−Re angles for the three XylNC ligands are close to 180° (range

Scheme 2. Redox Chemistry of **4** and **5** (R = Xyl)

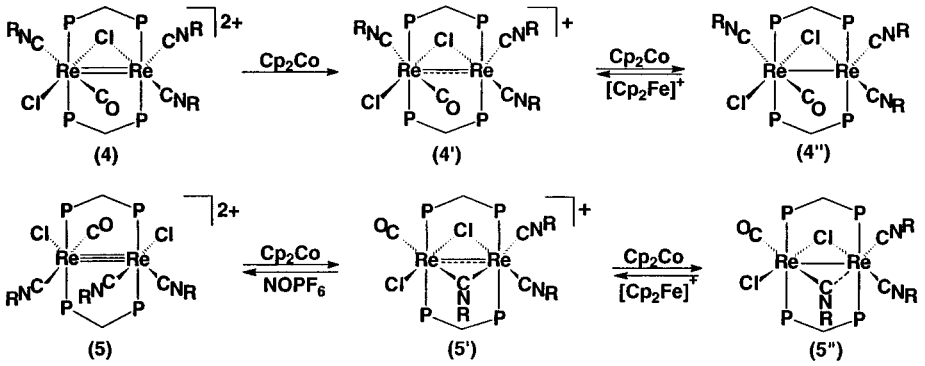

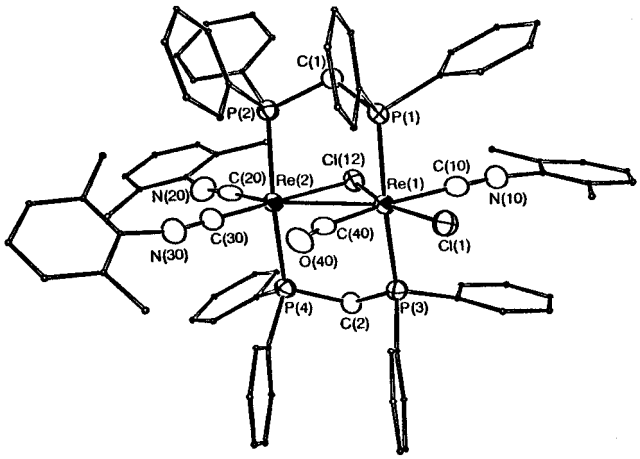

Figure 3. ORTEP[25] representation of the structure of the $Re_2Cl_2(\mu\text{-dppm})_2(CO)(CNXyl)_3$ molecule as present in **4″**. The thermal ellipsoids are drawn at the 50% probability level, except for the phenyl group atoms of the dppm ligands and the xylyl group atoms of the XylNC ligands, which are circles of arbitrary radius.

177−179°) while the C−N−C angles range from 160° to 173° with angles of 160.2(6)° and 161.4(6)° for the two XylNC ligands which are bound to Re(2). A weak Re−Re single bond is also present (Re(1)−Re(2) = 3.0442(7) Å), a feature which accords with an 18-electron count for each Re center and the observed diamagnetism of this neutral complex. Formally, oxidation of **4″** to **4** (via **4′**) involves the loss of two metal-based electrons and the conversion of the Re−Re singly bonded neutral complex to its doubly bonded dicationic congener. This bond order for **4** accords with an 18-electron count for the metal centers.

In comparing the IR spectral data for **4a**, **4a′**, and **4″** in Table 2, we note the expected shift of the ν(CN) modes to lower frequencies as the metal core is reduced and Re → π^*(XylNC) back-bonding increases. However, the ν(CO) mode occurs at an essentially constant frequency (ca. 1800 cm^{-1}). We suggest that the expected reduction in ν(CO) frequency as the dimetal core is reduced is effectively neutralized by changes in the nature of the weak unsymmetrical Re−CO···Re bridge that may be present. It is plausible that such a bridge weakens as reduction progresses. If Re(1) is the more easily reduced center of the two, then an increase in Re → π^*(CO) back-bonding at Re(1) would weaken the bridge and increase the interaction of CO with Re(1) at the expense of Re(2). Since these changes would only result in minor skeletal rearrangements, they would not affect the apparent reversibility of the electrochemical processes.

The reversibility of the electrochemical processes which are associated with the compounds **4a**, **4a′**, and **4″**, and the close structural similarity between these three oxidation states, stands in marked contrast to the redox chemistry of **5a** and **6a** (see Table 3). While **5a** and **6a** display two reversible-looking one-electron reductions in their cyclic voltammograms, with $E_{1/2}$ values of +0.30 and −0.43 V vs Ag/AgCl and +0.26 and −0.57 V vs Ag/AgCl, respectively, the products which result when these reductions are accessed chemically through the use of $(\eta^5\text{-}C_5H_5)_2Co$, viz., **5a′** and **5″**, and **6a′** and **6″**, respectively, are structurally quite different from **5a** and **6a** (see Schemes 2 and 3). This is demonstrated most clearly by a comparison of the CV's of **5a** and **5a′** (Figure 4), which shows them to be quite different. Similar differences exist between the CV's of **6a** and **6a′** (Table 3). The single-scan CV of **5a′** in Figure 4b shows that the irreversible oxidation at $E_{p,a}$ = ca. +0.8 V is followed by the rapid isomerization of the unstable species $\{\mathbf{5a'}\}^+$ back to **5a**, as seen by the appearance of the $E_{p,c}$ process at ca. +0.2 V. When a partial second scan is carried out (Figure 4b), with a switching potential of ca. −0.02 V, the $E_{p,a}$ process which is coupled to the process at $E_{p,c}$ = +0.21 V and is characteristic of the formation of **5a** is now observed, confirming that **5a′** isomerizes to **5a** once it has been oxidized. These conclusions are confirmed by the chemical oxidations we have carried out on solutions of **5a′**, **5″**, **6a′**, and **6″**, through the use of the oxidants $[(\eta^5\text{-}C_5H_5)_2Fe]PF_6$ and $NOPF_6$. These results, which are summarized in Schemes 2 and 3, demonstrate the chemical reversibility of all of the redox processes.

Although the NMR and/or IR spectral properties of the pairs of complexes **5a′**/**5″** and **6a′**/**6″** are generally rather similar, it is the very close similarity between their CV properties which confirms that a close structural relationship exists between these two series of compounds. Accordingly, it seems reasonable that the mechanism for the isomerization which interconverts **5a** with **5a′** and **6a** with **6a′** will be the same. One obvious possibility for this isomerization is shown in Scheme 2, where the first step in a "merry-go-round" process would convert an essentially open bioctahedral structure **5** to the proposed edge-sharing bioctahedral structure **5′**. While we have been unable to obtain X-ray quality single crystals of either **5a′** or **5″** to confirm this proposal, we have determined the structures of **6a′** and **6″** and found that the analogous process, when applied to **6a**, does lead to the observed structural isomerization. Accordingly, we are confident that the structures proposed for the monocation **5′** and the neutral complex **5″** in Scheme 2 are correct.

The ORTEP[25] representation of the cation present in **6a′** and the neutral molecule **6″** are shown in Figures 5 and 6. Both complexes have very similar structures which approach that of an edge-sharing bioctahedral geometry, the main difference being in the nature of the "bridging" XylNC ligand. The structural parameters for **6a′** and **6″** are compared in Table 5. The Re−Re distances for **6a′** and **6″** are 2.9777(8) and 3.0434(9) Å, respectively, which are consistent with formal bond orders

Scheme 3. Redox and Isomerization Chemistry of Complex **6** (R = Xyl)

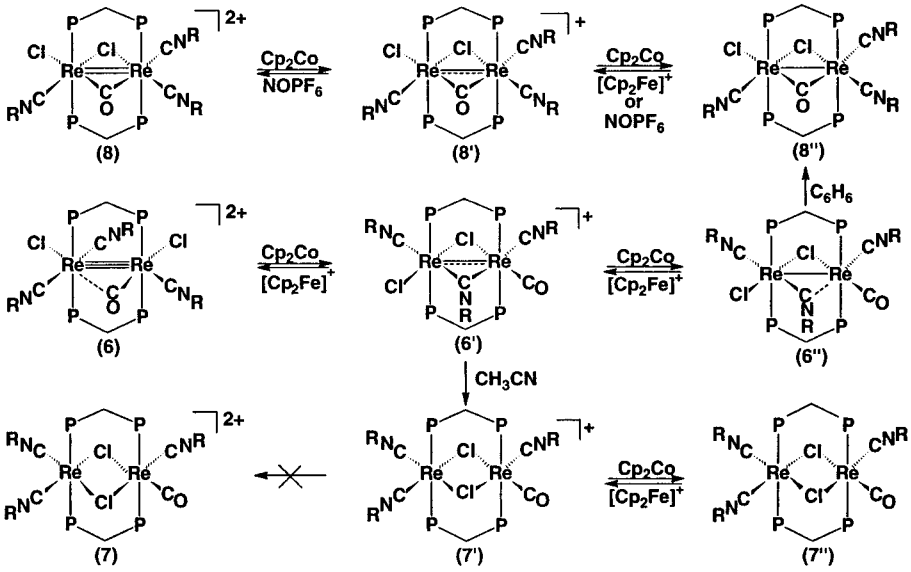

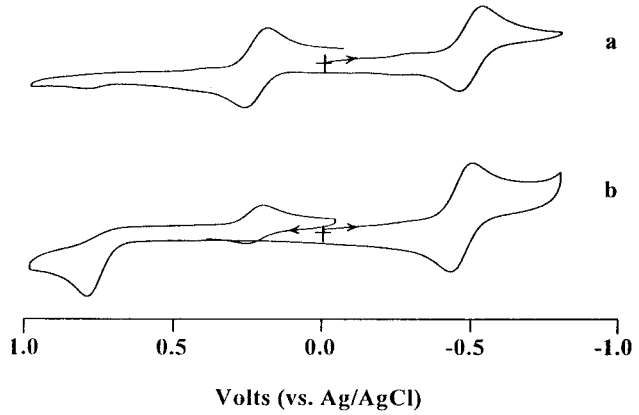

Figure 4. Cyclic voltammograms (scan rate 200 mV/s at a Pt bead electrode) in 0.1 M TBAH/CH_2Cl_2: (a) $[Re_2Cl_2(\mu\text{-dppm})_2(CO)(CNXyl)_3](O_3SCF_3)_2$ (**5a**); (b) $[Re_2Cl_2(\mu\text{-dppm})_2(CO)(CNXyl)_3]O_3SCF_3$ (**5a′**). For trace b a partial second scan shows that **5a** is the product of the irreversible oxidation of **5a′**. The CV trace for **5″** is identical to that shown in b for **5a′**.

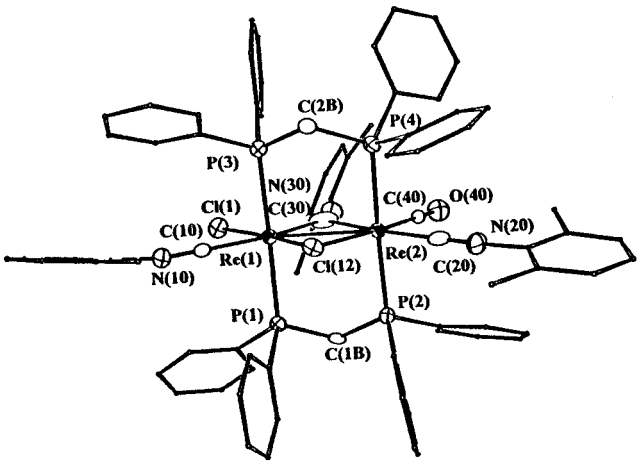

Figure 5. ORTEP[25] representation of the structure of the dirhenium cation $[Re_2Cl_2(\mu\text{-dppm})_2(CO)(CNXyl)_3]^+$ as present in **6a′**. This representation shows half of the disorder involving the terminal CO and Cl ligands (about a pseudo two-fold axis through the bridging atoms Cl(12) and C(30)). Disordered atoms not shown are Cl(2), C(50) and O(50). The thermal ellipsoids are drawn at the 50% probability level, except for the phenyl group atoms of the dppm ligands and the xylyl group atoms of the XylNC ligands, which are circles of arbitrary radius.

of 1.5 and 1; the bond order of 1 is in accord with an 18-electron count for the Re centers of **6″**. While the small magnitude of the decrease in Re−Re bond distance which accompanies the oxidation of **6″** to **6a′** is consistent with an increase in bond order, it could also be a consequence of removing an electron from an essentially nonbonding metal based orbital.

The principal structural differences between **6a′** and **6″** involve the XylNC ligand which is positioned to bridge the two metal centers. The distance Re(1)−C(30) is shorter by about 0.09 Å in the more highly reduced complex **6″**, and the angle N(30)−C(30)−Re(1) is larger by 13°. This results in an increase in the distance C(30)−Re(2) from 2.401(9) Å in **6a′** to ca. 2.65 Å in **6″** as the XylNC ligand transforms from being weakly bridging in the former complex to essentially terminally bound in **6″**. This trend is analogous to that we surmised took place in the sequence **4** → **4′** → **4″** (vide supra). Indeed, the structures of **6a′** and **6″** are similar to that determined for **4″**, the principal difference being the switch between "bridging" XylNC and CO ligands. The C−N−C angles for **6″** are appreciably smaller than for **6a′** (range 152−162° versus 165−172°), in accord with an increased degree of Re → π^*(XylNC) back-bonding in the former compound.

The crystal structures of the complexes **6a**, **6a′**, and **6″** are the first that have been obtained for a series containing the $[Re_2]^{4+}$, $[Re_2]^{3+}$, and $[Re_2]^{2+}$ cores; we have previously structurally characterized the series $[Re_2Cl_4(PMe_2Ph)_4]^{n+}$ (n = 2, 1, or 0), which contains the $[Re_2]^{6+}$, $[Re_2]^{5+}$, and $[Re_2]^{4+}$ cores.[26] Of special note is the change in formal Re−Re bond order from 3 to 1.5 to 1 as the dimetal core of **6a** is reduced to **6a′** and then **6′**, the biggest change accompanying the isomerization which takes place when **6a** is reduced to **6a′**.

During our successful attempts to grow single crystals of **6a′** and **6″** for their structure determinations, a variety of solvents and solvent mixtures were screened for this purpose. Mixtures of dichloromethane and diethyl ether proved suitable, whereas solutions of **6a′** in acetonitrile and **6″** in benzene produced crystals of the new isomeric forms **7a′** and **8″**, respectively, as shown in Scheme 3. These transformations, which occurred in

(26) Cotton, F. A.; Dunbar, K. R.; Falvello, L. R.; Tomas, M.; Walton, R. A. *J. Am. Chem. Soc.* **1983**, *105*, 4950.

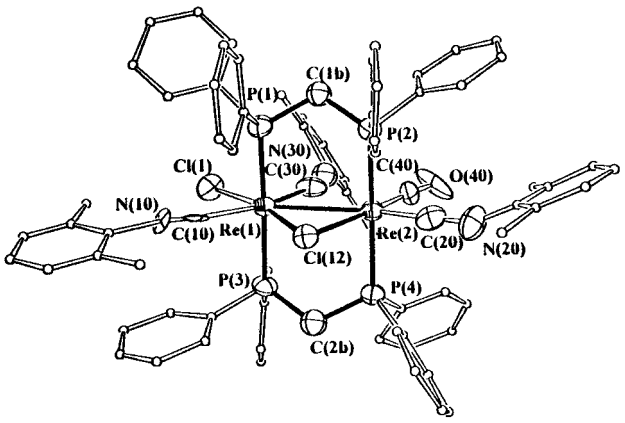

Figure 6. ORTEP[25] representation of the structure of one of the two independent molecules of $Re_2Cl_2(\mu\text{-dppm})_2(CO)(CNXyl)_3$ that are present in **6″**. The thermal ellipsoids are drawn at the 50% probability level, except for the phenyl group atoms of the dppm ligands and the xylyl group atoms of the XylNC ligands, which are circles of arbitrary radius.

good yield (>70%) at room temperature over periods of days or weeks, were found to be irreversible. The products **7a′** and **8″** were shown by IR and NMR spectroscopy (Table 2) and cyclic voltammetry (Table 3) to be structurally quite distinct from their precursors. Furthermore, the CV's of solutions of **7a′** and **8″** in 0.1 M TBAH/CH_2Cl_2 (Table 3) indicated that other oxidation states should be accessible. Through the use of $(\eta^5\text{-}C_5H_5)_2Co$ as a reductant and $[(\eta^5\text{-}C_5H_5)_2Fe]PF_6$ or $NOPF_6$ as an oxidant, we were able to obtain the neutral complex **7″** and $[PF_6]^-$ salts of the cations **8** and **8′**. This redox chemistry is summarized in Scheme 3 and was found to be reversible in all instances. The only compound we were unable to isolate was the dicationic species **7** when we reacted **7a′** with $NOPF_6$.

The structures of the redox pair **7a′**/**7″** were established by X-ray crystallography. The ORTEP[25] representations are given in Figures 7 and 8, while the most important structural parameters are compared in Table 6. A badly disordered triflate anion frustrated our attempts to obtain a high-quality structure of **7a′**. We note that in this edge-sharing bioctahedral di-μ-chloro bridged structure there is no Re−Re bond (the Re−Re distance is ca. 3.50 Å) and the three XylNC ligands are bound in a linear fashion with N−C−Re and C−N−C angles in the ranges 172−174° and 162−168°, respectively. The absence of any Re−Re bond implies that the odd electron is localized on one of the Re centers (presumably Re(2)) in this 17e/18e species. The reduction of **7a′** to **7″** should give a diamagnetic 18e/18e complex devoid of Re−Re bonding. This is the case as demonstrated by the structure determination of **7″**. The Re−Re distance is ca. 3.72 Å; for the second independent molecule, which is disordered about the inversion center, this distance is ca. 3.66 Å. The N−C−Re angles associated with the XylNC ligands are in the range 173−177°, but the C−N−C angles of the two XylNC ligands bound to Re(2) are smaller (147.4(10)° and 151.3(11)°) than that for the ligand bound to Re(1) (175.2-(13) Å). This accords with the more effective π-back-bonding acceptor capability of CO, which is bound to Re(1), compared to XylNC.

While we were unable to obtain good-quality single crystals of salts of **8**, **8′**, or the neutral isomer **8″**, the presence of a bridging carbonyl ligand is supported by IR spectroscopy, which shows a ν(CO) mode in the range 1770−1730 cm^{-1}. However, this frequency increases by 10−15 cm^{-1} for each unit decrease in oxidation state. As we discussed previously in the case of the series **4a**/**4a′**/**4″**, this counterintuitive order can be explained by changes in the nature of the carbonyl-bridge interaction involving the Re centers in these asymmetrical complexes.

The isomerization of **6a′** to **7a′** in acetonitrile (Scheme 3) occurs over a period of about 3 days and is unaffected by the presence of added *t*-BuNC or Cl^-; the *t*-BuNC ligand was added to ascertain whether a mixed XylNC/*t*-BuNC species would result. Accordingly, the mechanism for this isomerization does not appear to be dissociative in nature, but we have no further information on the mechanism of this reaction, or that of **6″** to **8″**, since we have not been able to isolate or detect any intermediates.

Table 5. Key Bond Distances (Å) and Bond Angles (deg) for the Dirhenium Cation $[Re_2Cl_2(\mu\text{-dppm})_2(CO)(CNXyl)_3]^+$ of **6a′** and the Molecule $Re_2Cl_2(\mu\text{-dppm})_2(CO)(CNXyl)_3$ of **6″** [a]

6a′ [b]		**6″** [c]	
Distances			
Re(1)−Re(2)	2.9777(8)	Re(1)−Re(2)	3.0434(9)
Re(1)−Cl(1)	2.390(5)	Re(1)−Cl(1)	2.470(4)
Re(1)−C(10)	2.017(7)	Re(1)−C(10)	2.12(2)
Re(1)−C(30)	2.124(8)	Re(1)−C(30)	2.033(17)
Re(1)−Cl(12)	2.4462(17)	Re(1)−Cl(12)	2.492(4)
Re(2)−C(40)	1.868(13)	Re(2)−C(40)	1.93(2)
Re(2)−C(20)	1.978(8)	Re(2)−C(20)	1.909(19)
Re(2)−C(30)	2.401(9)		
Re(2)−Cl(12)	2.4711(17)	Re(2)−Cl(12)	2.491(4)
Re(1)−P(1)	2.4547(18)	Re(1)−P(1)	2.385(4)
Re(1)−P(3)	2.4680(19)	Re(1)−P(3)	2.407(4)
Re(2)−P(2)	2.4113(18)	Re(2)−P(2)	2.383(4)
Re(2)−P(4)	2.4533(18)	Re(2)−P(4)	2.429(4)
C(10)−N(10)	1.148(8)	C(10)−N(10)	1.023(18)
C(20)−N(20)	1.162(9)	C(20)−N(20)	1.25(2)
C(30)−N(30)	1.173(9)	C(30)−N(30)	1.15(2)
C(40)−O(40)	1.143(19)	C(40)−O(40)	1.07(2)
Angles			
C(10)−Re(1)−C(30)	162.9(3)	C(30)−Re(1)−C(10)	160.1(6)
C(10)−Re(1)−Cl(1)	79.5(2)	C(10)−Re(1)−Cl(1)	79.4(5)
C(30)−Re(1)−Cl(1)	83.4(3)	C(30)−Re(1)−Cl(1)	80.8(5)
C(10)−Re(1)−Cl(12)	91.03(18)	C(10)−Re(1)−Cl(12)	88.8(4)
C(30)−Re(1)−Cl(12)	106.1(2)	C(30)−Re(1)−Cl(12)	111.1(5)
Cl(1)−Re(1)−Cl(12)	170.42(11)	Cl(1)−Re(1)−Cl(12)	167.30(15)
P(1)−Re(1)−P(3)	174.90(6)	P(1)−Re(1)−P(3)	175.87(16)
C(10)−Re(1)−Re(2)	144.11(17)	C(10)−Re(1)−Re(2)	141.0(4)
C(30)−Re(1)−Re(2)	53.0(2)	C(30)−Re(1)−Re(2)	58.9(5)
Cl(1)−Re(1)−Re(2)	136.40(10)	Cl(1)−Re(1)−Re(2)	139.63(11)
Cl(12)−Re(1)−Re(2)	53.11(4)	Cl(12)−Re(1)−Re(2)	52.33(9)
C(40)−Re(2)−C(20)	89.1(4)	C(20)−Re(2)−C(40)	88.5(7)
C(40)−Re(2)−C(30)	76.5(4)		
C(20)−Re(2)−C(30)	165.6(3)		
P(2)−Re(2)−P(4)	171.91(6)	P(2)−Re(2)−P(4)	174.31(16)
C(40)−Re(2)−Cl(12)	173.7(4)	C(40)−Re(2)−Cl(12)	167.7(5)
C(20)−Re(2)−Cl(12)	97.1(2)	C(20)−Re(2)−Cl(12)	103.4(5)
C(30)−Re(2)−Cl(12)	97.3(2)		
C(40)−Re(2)−Re(1)	121.5(4)	C(40)−Re(2)−Re(1)	116.0(5)
C(20)−Re(2)−Re(1)	149.2(2)	C(20)−Re(2)−Re(1)	155.3(5)
C(30)−Re(2)−Re(1)	45.0(2)		
Cl(12)−Re(2)−Re(1)	52.35(4)	Cl(12)−Re(2)−Re(1)	52.38(9)
Re(1)−Cl(12)−Re(2)	74.53(5)	Re(1)−Cl(12)−Re(2)	75.29(11)
N(10)−C(10)−Re(1)	174.6(6)	N(10)−C(10)−Re(1)	174.9(13)
N(20)−C(20)−Re(2)	178.4(6)	N(20)−C(20)−Re(2)	174.3(16)
N(30)−C(30)−Re(1)	148.1(7)	N(30)−C(30)−Re(1)	158.6(17)
N(30)−C(30)−Re(2)	129.8(7)		
Re(1)−C(30)−Re(2)	82.0(3)		
O(40)−C(40)−Re(2)	173.3(10)	O(40)−C(40)−Re(2)	170.5(17)
C(10)−N(10)−C(11)	171.7(7)	C(10)−N(10)−C(11)	162.0(17)
C(20)−N(20)−C(21)	170.1(8)	C(20)−N(20)−C(21)	152(2)
C(30)−N(30)−C(31)	165.9(8)	C(30)−N(30)−C(31)	161.1(18)

[a] Comparisons are made between corresponding parameters in the two structures as represented by the labeling schemes in Figures 5 and 6. Numbers in parentheses are estimated standard deviations in the least significant digits. Complete data are available as Supporting Information. [b] The CO ligand is disordered with the terminal chlorine atom. Data for one half of this disorder (as represented in Figure 5) is given. [c] Data provided for **6″** are for one of the two independent molecules in the asymmetric unit. Parameters for these molecules are essentially identical.

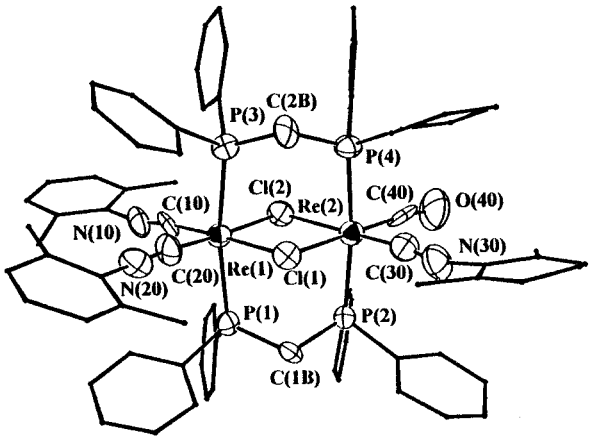

Figure 7. ORTEP[25] representation of the structure of the dirhenium cation $[Re_2Cl_2(\mu\text{-dppm})_2(CO)(CNXyl)_3]^{2+}$ as present in **7a′**. The thermal ellipsoids are drawn at the 50% probability level, except for the phenyl group atoms of the dppm ligands and the xylyl group atoms of the XylNC ligands, which are circles of arbitrary radius.

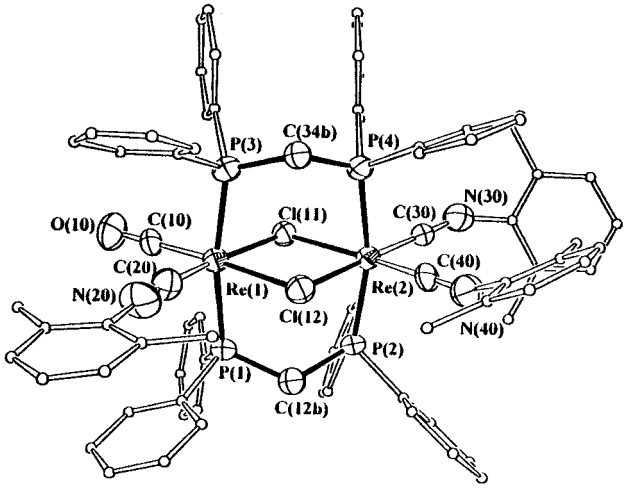

Figure 8. ORTEP[25] representation of the structure of one of the two independent molecules of $Re_2Cl_2(\mu\text{-dppm})_2(CO)(CNXyl)_3$ that are present in **7″**. The molecule shown is that which is located about a general position. The other molecule is disordered. The thermal ellipsoids are drawn at the 50% probability level, except for the phenyl group atoms of the dppm ligands and the xylyl group atoms of the XylNC ligands, which are circles of arbitrary radius.

Concluding Remarks

The remarkably varied isomer chemistry that has already been established for salts of the $[Re_2Cl_3(\mu\text{-dppm})_2(CO)(CNXyl)_2]^+$ cation[1,3−11] can be extended to the complex $[Re_2Cl_2(\mu\text{-dppm})_2(CO)(CNXyl)_3](O_3SCF_3)_2$, which has been isolated in three distinct, non-interconvertible isomeric forms (**4a**-**6a**) (Scheme 1). The solid state structures of these isomers are based upon open bioctahedra (**5a**) or are intermediate between open bioctahedra and edge-sharing bioctahedra (**4a** and **6a**). All three complexes display *reversible* redox chemistry, with two one-electron reductions being readily accessible (Schemes 2 and 3). In the case of **4a**, reductions to **4a′** and **4″** occur without structural rearrangement, whereas the first one-electron reductions of **5a** and **6a**, to **5a′** and **6a′**, respectively, are accompanied by isomerization to new bioctahedral structures. The second one-electron reductions to **5″** and **6″**, give compounds which are structurally similar to **5a′** and **6a′**. These coupled redox/isomerization processes, as well as the discovery that solutions of **6a′** and **6″** in acetonitrile and benzene slowly isomerize to additional isomeric forms (**7a′** and **8″**, respectively), reveal a dimension to the isomer chemistry of multiply bonded dirhenium compounds that contain the $[Re_2(\mu\text{-dppm})_2]$ moiety which we have not encountered in our previous studies of the $[Re_2Cl_3(\mu\text{-dppm})_2(CO)(CNXyl)_2]^+$ cation.[1,3−11]

The seven distinct structures we have established for the various isomers of $[Re_2Cl_2(\mu\text{-dppm})_2(CO)(CNXyl)_3]^{n+}$ ($n = 2$, 1, or 0) contain a wide variety of Re−Re bond orders, i.e., 3, 2, 1.5, 1, and 0. Studies of the chemical reactivities of the various isomeric forms **4**, **5**, **6**, **7**, and **8** toward various electrophiles and nucleophiles are underway.

Table 6. Key Bond Distances (Å) and Bond Angles (deg) for the Dirhenium Cation $[Re_2Cl_2(\mu\text{-dppm})_2(CO)(CNXyl)_3]^+$ of **7a′** and the Molecule $Re_2Cl_2(\mu\text{-dppm})_2(CO)(CNXyl)_3$ of **7″** [a]

7a′		**7″** [b]	
	Distances		
Re(1)−C(20)	1.91(2)	Re(2)−C(40)	1.885(10)
Re(1)−C(10)	1.95(2)	Re(2)−C(30)	1.886(10)
Re(1)−P(1)	2.452(5)	Re(2)−P(2)	2.422(3)
Re(1)−P(3)	2.450(5)	Re(2)−P(4)	2.394(3)
Re(1)−Cl(1)	2.463(5)	Re(2)−Cl(12)	2.541(3)
Re(1)−Cl(2)	2.465(5)	Re(2)−Cl(11)	2.529(3)
Re(2)−C(30)	1.85(2)	Re(1)−C(20)	1.943(12)
Re(2)−C(40)	1.94(3)	Re(1)−C(10)	1.882(10)
Re(2)−P(2)	2.401(5)	Re(1)−P(1)	2.398(3)
Re(2)−P(4)	2.405(5)	Re(1)−P(3)	2.390(3)
Re(2)−Cl(1)	2.533(5)	Re(1)−Cl(12)	2.536(3)
Re(2)−Cl(2)	2.536(5)	Re(1)−Cl(11)	2.526(3)
C(10)−N(10)	1.12(2)	C(30)−N(30)	1.203(12)
C(20)−N(20)	1.15(2)	C(40)−N(40)	1.190(12)
C(30)−N(30)	1.19(3)	C(20)−N(20)	1.144(13)
C(40)−O(40)	1.13(2)	C(10)−O(10)	1.151(11)
	Angles		
C(20)−Re(1)−C(10)	93.1(8)	C(40)−Re(2)−C(30)	84.8(4)
P(3)−Re(1)−P(1)	169.47(17)	P(4)−Re(2)−P(2)	166.64(9)
C(20)−Re(1)−Cl(1)	85.9(7)	C(40)−Re(2)−Cl(12)	87.1(3)
C(10)−Re(1)−Cl(1)	177.4(5)	C(30)−Re(2)−Cl(12)	171.4(3)
C(20)−Re(1)−Cl(2)	175.8(7)	C(40)−Re(2)−Cl(11)	172.2(3)
C(10)−Re(1)−Cl(2)	88.4(5)	C(30)−Re(2)−Cl(11)	102.6(3)
Cl(1)−Re(1)−Cl(2)	92.71(17)	Cl(11)−Re(2)−Cl(12)	85.36(10)
C(30)−Re(2)−C(40)	88.0(8)	C(10)−Re(1)−C(20)	87.5(4)
P(2)−Re(2)−P(4)	173.08(18)	P(3)−Re(1)−P(1)	169.08(9)
C(30)−Re(2)−Cl(1)	87.0(7)	C(10)−Re(1)−Cl(12)	175.0(3)
C(40)−Re(2)−Cl(1)	174.6(6)	C(20)−Re(1)−Cl(12)	87.6(3)
C(30)−Re(2)−Cl(2)	175.9(7)	C(10)−Re(1)−Cl(11)	99.4(3)
C(40)−Re(2)−Cl(2)	95.5(5)	C(20)−Re(1)−Cl(11)	173.1(3)
Cl(1)−Re(2)−Cl(2)	89.42(16)	Cl(11)−Re(1)−Cl(12)	85.52(10)
Re(1)−Cl(1)−Re(2)	88.99(16)	Re(1)−Cl(12)−Re(2)	94.26(10)
Re(1)−Cl(2)−Re(2)	88.87(16)	Re(1)−Cl(11)−Re(2)	94.79(10)
N(10)−C(10)−Re(1)	173.1(18)	N(30)−C(30)−Re(2)	173.0(9)
N(20)−C(20)−Re(1)	174(2)	N(40)−C(40)−Re(2)	177.6(10)
N(30)−C(30)−Re(2)	172(2)	N(20)−C(20)−Re(1)	174.5(11)
O(40)−C(40)−Re(2)	172.7(18)	O(10)−C(10)−Re(1)	177.3(10)
C(10)−N(10)−C(11)	167(2)	C(30)−N(30)−C(31)	147.4(10)
C(20)−N(20)−C(21)	168(2)	C(40)−N(40)−C(41)	151.3(11)
C(30)−N(30)−C(31)	162(2)	C(20)−N(20)−C(21)	175.2(13)

[a] Comparisons are made between corresponding parameters in the two structures as represented by the labeling schemes in Figures 7 and 8. Numbers in parentheses are estimated standard deviations in the least significant digits. Complete data are available as Supporting Information. [b] Data provided for **7″** are for one of the two independent molecules in the asymmetric unit. The second molecule is located about an inversion center and is disordered such that the CO ligand atoms are indistinguishable from the C and N atoms of the three XylNC ligands (see the Experimental Section for a full discussion).

Acknowledgment. This work was supported in part by the National Science Foundation (Grant No. CHE94-09932).

Supporting Information Available: X-ray crystallographic files in CIF format for complexes **4″**, **5a**, **6a**, **6a′**, **6″**, **7a′**, and **7″**. This material is available free of charge via the Internet at http://pubs.acs.org.

IC981192Q